Quasiclassical negative magnetoresistance of a two-dimensional electron gas in a random magnetic field

A. A. Bykov,* G. M. Gusev, and J. R. Leite
Instituto de Física da Universidade de São Paulo, CP 66318CEP 05315-970, São Paulo, SP, Brazil

A. K. Bakarov, A. V. Goran, V. M. Kudryashev, and A. I. Toropov
Institute of Semiconductor Physics, Novosibirsk, Russia

(Received 15 August 2001; revised manuscript received 20 September 2001; published 11 December 2001)

We have studied negative magnetoresistance of a nonplanar two-dimensional electron gas. Effectively due to the curved AlGaAs/GaAs interface, electrons see a uniform in-plane magnetic field B as a random magnetic field (RMF). Small additional perpendicular B leads to a negative magnetoresistance predicted by a semiclassical treatment of the RMF problem beyond the relaxation-time approximation, in accordance with our observations.

DOI: 10.1103/PhysRevB.65.035302 PACS number(s): 73.50.Jt, 72.20.My, 75.70.−i

The low-field magnetotransport properties of a two-dimensional electron gas (2DEG) have a great impact on the investigation of quantum phenomena. The most prominent effect is a negative magnetoresistance (MR) induced by the suppression of quantum interference corrections to the conductivity by the magnetic field.[1] Quasiclassical approximation demonstrated that the longitudinal resistivity ρ_{xx} is independent of the magnetic field in the limit of white-noise disorder. However, recently the quasiclassical transport properties of a 2DEG have been reexamined because of the inconsistency with the several experimental observations. In particular, a pronounced positive MR has been observed near half-filling $\nu=1/2$ of the lowest Landau level.[2] The transport properties of the strongly correlated electrons in the lowest Landau level can be described in terms of the composite fermions moving in a random magnetic field (RMF) with zero average at half-filling.[3] Away from $\nu=1/2$, the composite fermions experience the effective magnetic field $B_{eff}=B-B_{1/2}$, where $B_{1/2}=2(hc/e)n_s$, where n_s is the electron density. Therefore, the magnetotransport near $\nu=1/2$ is related to the problem of electron transport in a RMF.

Motivated by this problem, the magnetoresistance of this system has been calculated in a numbers of papers.[4–6] It was argued that the semiclassical approach is probably a more adequate treatment of the RMF scattering, because the effects of the quantum interference are suppressed. In addition, the correlation length of the RMF ξ is much larger than the Fermi wavelength of the electrons λ_F. In the regime of a weak RMF, which means that $\alpha=\xi/R_0\ll 1$, where $R_0=hmc/(e\lambda_F B_0)$ and B_0 is the average amplitude of the RMF, theory predicts a strong positive MR,[5,6] in agreement with experimental data.[2] In the strong-RMF regime, when $\alpha\gg 1$, a negative classical MR has been predicted.[4,7] The CF description of the vicinity of $\nu=1/2$ of the lowest Landau level is probably more relevant to the moderately small $\alpha\approx 0.2$–0.5, therefore the strong-RMF regime cannot be realized in such a system, and negative MR is not observed. Other methods to create a RMF consist of attaching superconducting or ferromagnetic films over the heterostructures with 2DEG.[8,9]

Recently, 2DEG grown on nonplanar prepatterning GaAs substrates has been used to produce a nonuniform magnetic field.[10,11] Due to the interface roughness the 2DEG sees an external uniform in-plane magnetic field B_{ext} as a random perpendicular magnetic field. For a magnetic field oriented parallel to the substrate, the normal component of B can be expressed as $B_N\approx\pm(a/d)B_{ext}$, where a is the height of the roughness, d is the average periodicity of the surface corrugations, and $a/d\ll 1$. The parameter α can be rewritten as $\alpha=a\lambda_F B_{ext}/\Phi_0$, where $\Phi_0=hc/e$ is the magnetic-flux quantum, since $d\sim\xi$. For corrugation height $a=300$ Å (see Ref. 12) we obtain $\alpha=0.24B_{ext}$ (T). Therefore, the strong-RMF regime can be approached at $B\simeq 5$ T. When the external magnetic field is tilted away from the substrate plane, an additional perpendicular component of the magnetic field appears. It allows to study the MR in a strong-RMF regime in the presence of the weak uniform external perpendicular field B.

In this paper we present the results of transport measurements on the samples with 2DEG grown on the prepatterned nonplanar GaAs substrate. We observe the strong positive MR as a function of the in-plane magnetic field. This is consistent with the quasiclassical treatment of the transport in a RMF with zero average and is attributed to the electron scattering by magnetic-field inhomogeneities in the weak-RMF regime and formation of the snakelike trajectories in the strong-RMF regime.[13] When the magnetic field is slightly tilted away from the substrate plane, the resistance in a strong parallel field decreases. This behavior is consistent with prediction of a classical negative magnetoresistance in the presence of the RMF and weak uniform perpendicular B.[4,7]

Samples were fabricated employing overgrowth of GaAs and $Al_xGa_{1-x}As$ materials by molecular-beam epitaxy on prepatterned GaAs substrates. Figure 1(a) shows the atomic force image of the sample surface after regrowth. Because the 2DEG is buried close to the surface, it has the same topography. Figure 1(b) shows the magnetic-field modulation for the nonplanar 2DEG confined near this surface, when uniform magnetic field is applied parallel to the substrate

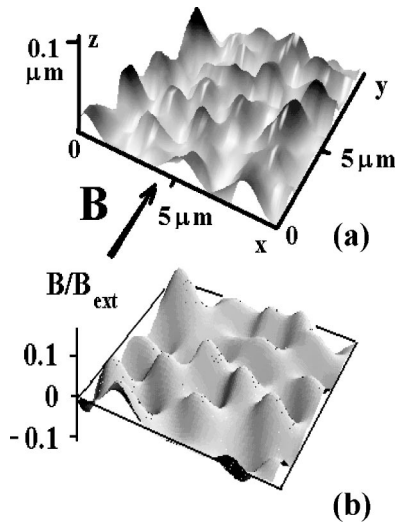

FIG. 1. (a) Atomic force microscope image of the sample surface. (b) Magnetic-field profile calculated for the surface profile shown in Fig. 1(a) when the in-plane magnetic field is oriented along the *y* direction.

plane in the direction perpendicular to the current (*y* axis). We can see that the magnetic field has long-range character. We also calculated the spatial profile of the RMF for the realistic sample surface shown in Fig. 1, when the external in-plane magnetic field was directed along the *x* or *y* axis, shown in Fig. 2. One might see here that for the sample geometry, when the in-plane field was oriented along the *y* axis, the effective magnetic field has a really random character, and $B(r)=0$ lines are closed and form a square network (Fig. 2, top). On the other hand, when the magnetic field was oriented along the *x* axis, $B(r)=0$ lines are directed along the *y* axis, and the effective magnetic field forms magnetic barriers across the current flow (Fig. 2, bottom). Anisotropy of the surface irregularities after regrowth has been already reported in Ref. 14 and can be explained by the dependence of GaAs growth velocity on the crystal directions. Depending on the substrate etching and the GaAs buffer layer thickness it is possible to obtain variety of the surface configurations between ''stripelike'' and ''hilllike'' structures.[11,12,14] However, this method does not permit to grow samples with an absolutely isotropic structured surface due to the orientation-dependent properties of the GaAs material. We compare the profile of the effective magnetic field with the correlator, which is usually used in different theories describing transport properties of 2D electrons in a random magnetic field:[4,6]

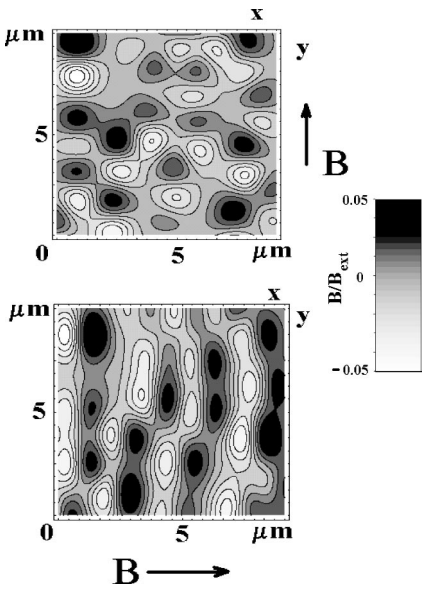

FIG. 2. Spatial profile of the random magnetic field for the realistic sample surface shown in Fig. 1, when the in-plane magnetic field is directed along the *y* axis (top) and *x* axis (bottom).

$$F(r)\approx\langle B(0)B(r)\rangle\approx B_0^2/(1+r^2/4\xi^2)^{3/2}. \tag{1}$$

We can see that the correlator $F(r)$ in the true RMF model is characterized by a single spatial scale, which is the correlation length of the magnetic field. For realistic profiles, the correlator can be direction dependent. From the comparison of the experimental data and Eq. (1) we derived $B_0\approx(0.06\pm0.02)B_{ext}$ and the single correlation length $\xi\approx0.6\pm0.2$ μm only for the geometry, when the external in-plane magnetic field was oriented along the *y* axis (Fig. 2, top). For the magnetic field directed along the *x* axis the magnetic profile is not described by the correlator with a single scale parameter. However, we find that the correlator in the *x* direction $F(x,y=\text{const})$ can be characterized by $\xi_x\approx0.6\pm0.2$ μm with approximately the same amplitude B_0. On the other hand $F(y,x=\text{const})$ strongly depends on the coordinate *x*. Therefore we may conclude here that the true RMF profile is realized for the geometry when the in-plane field is oriented in a direction perpendicular to the current, and it will cause the expected anisotropic behavior of the magnetoresistance in this case. Details of the sample preparation are reported in Ref. 14. We note that the surface is more irregular, and the corrugation height is larger than in the samples studied in Ref. 14. The mobility of the nonplanar 2DEG is $(40-50)\times10^3$ cm^2/V s, and the electron density is $n_s=5.5\times10^{11}$ cm^{-2} at $T=4.2$ K. The mobility in samples studied here is smaller than in the previously investigated structures.[11,12,14] We attribute this fact to the scattering by the interface roughness, which is consistent with the more irregular character of the surface in these samples. The mean free path at $B=0$ l_0 is 0.8 μm, which is comparable with the correlation length of the random magnetic field. This value agrees with our suggestion that the major scattering mechanism at $B=0$ is the scattering by the surface corrugations. Structures studied in Refs. 11, 12, and 14 have a regular stripelike 2DEG shape, and therefore cannot be used for the study of the classical MR in the weak uniform and strong random magnetic field. The nonplanar surface is situated on one side of the Hall bar. The distance between voltage probes was 100 μm, and the width of the bar was 50 μm. Resistance is measured between voltage probes 2 and 3 (or 7 and 8), as is shown in Fig. 3. Another side of the Hall bar contains the conventional planar 2DEG, and its properties were compared with transport properties of electrons in an effective RMF. We also used the Hall voltage of the planar 2DEG

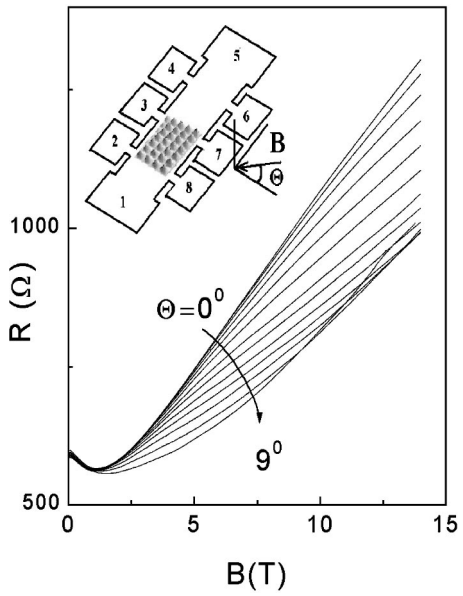

FIG. 3. Magnetoresistance as a function of the magnetic field for different angles Θ between the applied magnetic field and plane of the substrate at $T=4.2$ K. The in-plane magnetic-field component is directed along the y axis, perpendicular to the current flow. Inset: schematic view of the sample and experiment geometry.

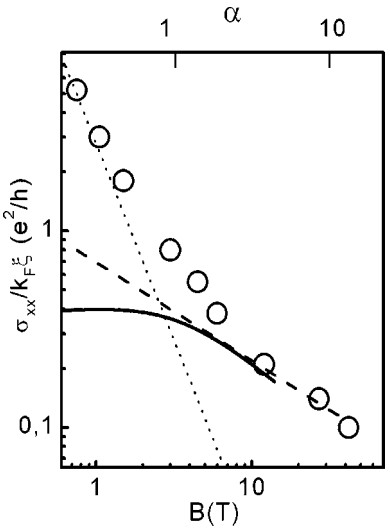

FIG. 4. Conductivity as a function of the in-plane magnetic field. The dotted and the dashed lines correspond to the theoretical asymptotic behavior given by expressions (2) and (6), respectively, for the conductivity in a random magnetic field as a function of the parameter α. Circles are results of the numerical simulations according to Ref. 13.

for the measurements of the tilt angle with precision of 0.02°. The measurement temperature was 1.5–4.2 K. We study three samples with identical parameters, which demonstrate similar results.

Figure 3 shows the longitudinal magnetoresistance $R_{xx}(B)$ when the applied magnetic field is exactly parallel to the substrate, and when B is slightly tilted away from the substrate plane. We can see strong positive magnetoresistance. However, at a relatively small tilt angle Θ the amplitude of the magnetoresistance $\Delta R_{xx}=R_{xx}(B)-R_{xx}(0)$ decreases with Θ. In the reference planar sample the MR was smaller than 1%. We have to note that in the tilted field a small additional perpendicular component of the magnetic field is applied to the 2DEG. The strong positive magnetoresistance in parallel field we attribute to the RMF scattering. As we already mentioned above, the amplitude of the RMF is proportional to the external parallel field. The conductivity in the weak-RMF regime is given by[15]

$$\sigma_{xx}=(2e^2/h)(2\pi\xi/4\alpha^2\lambda_F)\sim B_{ext}^{-2}. \tag{2}$$

In the strong-RMF regime the conductivity is determined by the percolation of the snakelike trajectories, which move along $B(r)=0$ lines. Such trajectories form a network, and in the semiclassical limit the conductance of the square network at short distances can be expressed as[15]

$$\sigma_{xx}=(2e^2/h)M, \tag{3}$$

where $M=k_F W/\pi$ is the number of snakelike channels propagating along the zero-field contours in the same direction, where k_F is the Fermi vector, and W is the width of the effective magnetic potential. In accordance with the semiclassical picture of the electron motion in a nonuniform linear-step magnetic field we have[16]

$$W=\Lambda(2k_F\Lambda)^{1/2}, \tag{4}$$

where $\Lambda=(h\nabla B/e)^{1/3}$, and ∇B is the magnetic-field gradient. Substituting Eqs. (4) into (3) we obtain

$$\sigma_{xx}\approx(2e^2/h)(k_F\Lambda)^{3/2}\sim B_{ext}^{-1/2}. \tag{5}$$

Detailed analysis of the conductivity demonstrated the importance of the critical saddle points, when snake states can cross over from one zero-field line to another.[13] This model predicts the following behavior of the conductivity in a RMF with a zero average:

$$\sigma_{xx}=(2Ce^2/h)(k_F\xi/\alpha^{1/2})(\ln\alpha)^{1/4}\sim B_{ext}^{-1/2}, \tag{6}$$

where C is the coefficient that can be found from the numerical simulation. Figure 4 shows the experimental dependence of the magnetoconductivity, recalculated from the magnetoresistance curve for $\Theta=0°$, and numerical results for σ_{xx} taken from Ref. 13. We can see that the asymptotic behavior of the conductivity $\sigma_{xx}\sim\alpha^{-1/2}$ for $\alpha\gg1$ is consistent with our experimental observation. In low magnetic field $B<3$ T the impurity scattering becomes dominant. We did not attempt to calculate magnetic scattering mechanisms for arbitrary magnetic fluctuations, since we are only interested in the strong-RMF approximation. In our samples the mean free path at zero field l_0 is comparable with the correlation length of the RMF, therefore the scattering by the interface corrugation (or impurity) may play some role in the strong parallel magnetic field. However, as we already mentioned above, the major scattering mechanism in the RMF is the reflection of the snake states by critical saddle points, where snake states can cross from one $B(r)=0$ line to another.[13,15]

Impurity scattering should be suppressed in the strong-RMF regime when $R_0 < l_0$ due to the mechanism similar the one considered in the quantum Hall-effect regime for edge states.[17] In this case the edge states scattered by impurity continue to follow the edge. In the random magnetic field the snake state scattered by impurity will continue to follow the $B(r)=0$ line. The drifting cyclotron trajectories, which move along the closed magnetic-field contours, are localized and do not contribute to the conductivity in the presence of the impurity scattering, since $R_0 < l_0$. Therefore, we believe that transport properties in the presence of the strong in-plane external magnetic field are determined by the percolation of the snakelike states in the RMF, and impurity scattering is not important. It is seen in Fig. 3 that the strong-RMF regime is approached at $B \approx 3.3$ T, when $\alpha = 1$, which corresponds to $B_0 \simeq 0.06 B_{ext}$ in agreement with our estimations of the amplitude of the magnetic-field fluctuations (Fig. 2). It is worth mentioning that we did not find any temperature dependence of the magnetoresistance in the temperature interval 1.5–4.2 K. In zero magnetic field weak-localization effects are responsible for the increase of the resistance with decreasing temperature. Since the conductivity in a strong RMF is determined by the snake states, one might expect that interference effects between snakelike trajectories would lead to the quantum localization. However, chirality of the snake states excludes the interference between the pairs of time-reversed paths, which contributes to the weak localization in the random impurity potential in zero magnetic field. Therefore, it was argued that all states in the RMF are delocalized.[18] On the other hand in a mean-field treatment, one obtains quantum interference due to the scattering process in the saddle points of the percolation network. Such scattering leads to the random-phase shift and the mixing of the snake states along the $B(r)=0$ line, and therefore it was concluded that all states in the RMF are localized.[15,19] Further theoretical investigations and measurements at lower temperature are necessary to resolve the problem of localization of 2D electrons in a random magnetic field. Absence of the T dependence supports our suggestion that the magnetoresistance in our system has a classical origin.

To finish part of the work concerning the measurements in a parallel magnetic field, we have to mention that in low B we also observe small negative magnetoresistance (Fig. 3). We attribute this effect to the negative MR, which was first observed in a random antidot lattice in a perpendicular magnetic field,[20] and has been calculated recently in Ref. 21. It has been demonstrated that quassiclasical memory effects in a 2DEG in the presence of the random array of antidots and long-range disorder due to impurities lead to the negative classical magnetoresistance. Due to the nonplanar interface profile the electron density is probably slightly inhomogeneous, which is equivalent to the presence of an additional random long-range electrostatic potential. Since the surface corrugations are similar to hard-wall scatters, like antidot, one would expect such a negative MR in our system. Because the one source of MR is the bending of the electron trajectory by the magnetic field, we believe that the magnetic-field orientation is not very important in this case, since in parallel external B, the normal component of B in a curved 2DEG within the correlation domain may be different from zero. This conclusion is supported by the measurements in a perpendicular magnetic field. In this geometry we also observe negative MR in a low magnetic field, similar to that previously reported in stripe-shaped 2DEG.[12] However, we should emphasize here that the origin of such negative magnetoresistance and MR in the random magnetic field studied in our paper is different.

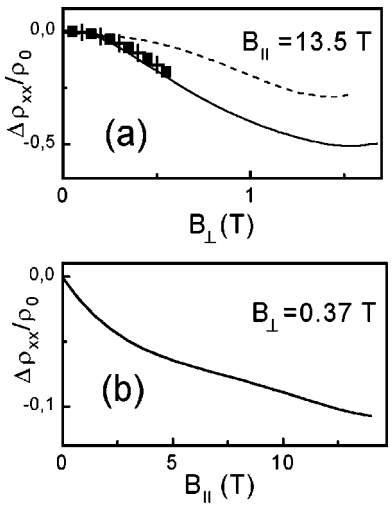

FIG. 5. (a) Magnetoresistivity as a function of the magnetic-field component perpendicular to the substrate at $B_{||}=13.5$ T. The solid line: experimental data recalculated from the curves, shown in Fig. 3, dashes: magnetoresistivity in the random magnetic field obtained from the numerical simulations [from Eqs. (9), (10), and (16)], squares: Eq. (17), and crosses: Eq. (18). (b) Experimental magnetoresistivity as a function of the in-plane magnetic field at $B_\perp = 0.37$ T, obtained from the curves shown in Fig. 3.

We now turn to the experiments in the tilted magnetic field shown in Fig. 3. Since the condition of the strong RMF is met in the experiments, we can compare our results with predictions made in Refs. 4 and 7. Figure 3 shows that the resistance at $B=14$ T decreases with tilt angle, or with an additional perpendicular component of the magnetic field. In order to obtain $\Delta R_{xx}/R_0$ in the RMF as a function of the perpendicular $B_\perp$ we should subtract resistance $R_{xx}(B_{||})$ measured at $\Theta = 0°$ and dependencies $R_{xx}(B_{||})$ measured at different angles, therefore $\Delta R_{xx}(B_{||},\Theta) = R_{xx}(B_{||},\Theta) - R_0(B_{||})$. Since $B_\perp = B_{ext}\sin\Theta$, and $B_{||} = B_{ext}\cos\Theta$, we can recalculate the relative magnetoresistance $\Delta R_{xx}/R_0$ (or magnetoresistivity $\Delta\rho_{xx}/\rho_0$) versus $B_\perp$ at a constant $B_{||}$ [Fig. 5(a)] and MR versus $B_{||}$ at a constant $B_\perp$ [Fig. 5(b)]. We can see large negative magnetoresistance in both cases. One of the important questions might be whether the observed negative MR is due to the RMF effect, or if it results from MR in a low perpendicular magnetic field and can be explained by ''hard-wall scatters plus the long-range potential'' mechanism considered in Ref. 21, which we discussed above. First, we can argue here in favor of the RMF mechanism, in which parallel B changes dramatically the properties of the 2DEG in comparison with zero magnetic field, where, in particular, as we discussed above, electron trajectories transform into snakelike orbits. In this case the ''hard-wall

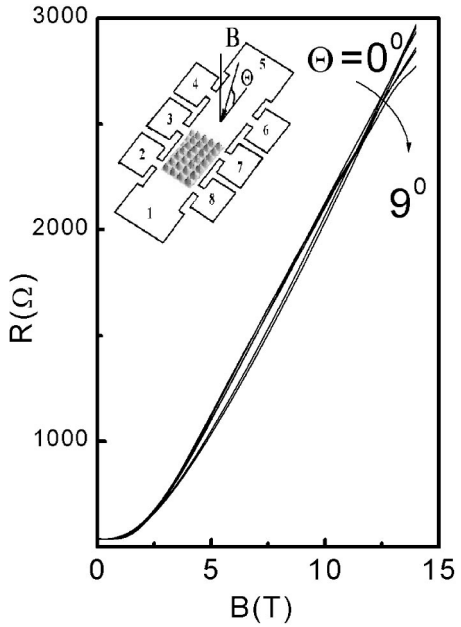

FIG. 6. Magnetoresistance as a function of the magnetic field for different angles Θ between the applied magnetic field and the plane of the substrate at $T=4.2$ K. The in-plane magnetic-field component is directed along the *x* axis, parallel to the current. Inset: schematic view of the sample and experiment geometry.

scatters plus long-range potential'' mechanism is not more valid at $B=14$ T. Second we perform additional measurements justifying that the presence of the RMF is an essential point for the existence of the negative MR in a strong parallel magnetic field. Figures 1 and 2 show that the in-plane magnetic field was directed along the *y* axis. Figure 6 shows also the results of the measurements for the geometry when the in-plane magnetic field was directed along the *x* axis. We can see that the resistance increases with *B* from 580 to 3000 Ω, a ratio of 5, which is almost two times larger than for the geometry, when the applied magnetic field was directed along the *y* axis (Fig. 3). We can see also that the magnetoresistance does not depend on the tilt angle, when Θ varies from 0° to 9°. From the computer simulation of the effective magnetic-field profile, which is shown in Fig. 2 (bottom), we can see that when the magnetic field was oriented along the *x* axis, and no negative MR is found, $B(r)=0$ lines are directed along the *y* axis, and the effective magnetic field forms magnetic barriers across the current flow. Such magnetic barriers should lead to larger positive MR than the RMF square network configuration. Magnetoresistance in the magnetic barrier configuration has been calculated in Refs. 22 and 23, and only large positive MR has been predicted. Therefore, it is reasonable to suggest, that for the observation of the negative MR, a really random magnetic-field configuration is necessary. The absence of the negative MR in the ''magnetic barrier'' experimental geometry supports our assumption about the origin of the negative MR in RMF geometry, shown in Fig. 3. Certainly, if the negative MR results from the ''hard-wall scatters plus long-range potential'' mechanism, it should be observed for all orientations of the magnetic field, which disagrees with our observations. Therefore, we attribute the appearance of the negative MR in the strong parallel field and small additional $B_\perp$ to the RMF mechanism considered in Refs. 4 and 7.

Now, let us compare the theoretical calculations and experimental data. The Boltzmann transport theory describes the magnetotransport properties of the metals by the semiclassical equations based on the relaxation-time approximation. In particular, the longitudinal σ_{xx} and diagonal σ_{xy} conductivities in magnetic field $B_\perp$ for an isotropic system have the Drude form

$$\sigma_{xx}(B)=\sigma_0/[1+(\omega_c\tau)^2], \tag{7}$$

$$\sigma_{xy}(B)=\sigma_0(\omega_c\tau)/[1+(\omega_c\tau)^2], \tag{8}$$

where $\sigma_0=e^2n_s\tau_{tr}/m$, $\omega_c=eB_\perp/cm$ is the cyclotron frequency, *m* is the effective mass, n_s is the electron concentration, and τ_{tr} is the transport scattering time. The resistivity can be obtained by inverting the conductivity tensor:

$$\rho_{xx}(B)=\sigma_{xx}/(\sigma_{xx}^2+\sigma_{xy}^2). \tag{9}$$

Deviations of the resistivity from the constant in the magnetic field usually is defined as

$$\Delta\rho_{xx}(B)=\rho_{xx}(B)-\rho_0, \tag{10}$$

where $\rho_0=1/\sigma_0$. The use of Eqs. (7)–(9) yields the magnetoresistivity in the low magnetic field:

$$\Delta\rho_{xx}(B)/\rho_0\approx-[\Delta\sigma_{xx}(B)/\sigma_{xx}(B)]-[\sigma_{xy}(B)/\sigma_{xx}(B)]^2, \tag{11}$$

where $\Delta\sigma_{xx}(B)=\sigma_{xx}(B)-\sigma_0$. Substituting Eqs. (7) and (8) into (11) we can see that the first and second terms of expression (11) exactly cancel out and result in zero MR. This is due to the fact that the decrease of the mean free path in the presence of the Lorentz force is exactly compensated by the Hall effect. Equation (11) can be rewritten in terms of the relaxation-time approximation:

$$\Delta\rho_{xx}(B)/\rho_0\approx\omega_c^2[\langle\tau_{tr}^2\rangle-\langle\tau_{tr}\rangle^2], \tag{12}$$

where $\langle\tau_{tr}\rangle=1/\tau_{tr}\int_0^\infty[t\exp(-t/\tau_{tr})]dt$,

$$\langle\tau_{tr}^2\rangle=1/2\tau_{tr}\int_0^\infty[t^2\exp(-t/\tau_{tr})]dt. \tag{13}$$

We can see that in this case $\langle\tau_{tr}^2\rangle=\langle\tau_{tr}\rangle^2$, and the longitudinal resistivity is independent of the magnetic field. As we already mentioned above, it has been demonstrated that a semiclassical treatment of the RMF scattering beyond the relaxation-time approximation leads to the negative MR in the presence of the additional uniform magnetic field. In particular, it has been shown that Eq. (13) for the transport scattering time should be rewritten in the form[4]

$$\langle\tau_{tr}\rangle=1/\tau_{tr}\int_0^\infty dt\left[t\exp\left(-\int_0^t(t-t')F(t')dt'\right)\right], \tag{14}$$

where *F* is the correlator of the RMF, given by Eq. (1). One might see that the exponential factor in Eq. (14) is not exactly proportional to *t*, but at small *t* behaves as t^2, therefore

$\langle \tau_{tr}^2 \rangle \neq \langle \tau_{tr} \rangle^2$. Detailed calculations performed in Ref. 4 give a larger negative contribution to the MR of the relative magnitude

$$\Delta\rho_{xx}(B)/\rho_0 \approx -C_1(\omega_c\tau_{tr})^2 \tag{15}$$

at $\omega_c\tau_{tr} \ll 1$, where the numerical factor C_1 depends on the realistic RMF configuration. We estimate the transport scattering time in the RMF from the simple equation $\tau_{tr}=\xi/v_F$ and obtain $\omega_c\tau_{tr}\approx 1$ at $B_\perp \sim 0.2-0.4$ T. As was mentioned in Ref. 4, the MR may change sign at $\omega_c\tau_{tr}\approx 1$ and remain positive in the strong magnetic field. Figure 3 shows that resistance decreases with tilt angles, but for high fields and angles $\Theta > 9°$ starts to increase. It agrees with theoretical predictions,[4] however, semiclassical analysis becomes insufficient at strong field, therefore we did not attempt to measure MR at tilt angles $\Theta > 9°$. In order to compare our results with theory in the larger $B_\perp$ range, we performed the numerical simulation of the conductivity tensor in the RMF. According to Refs. 4 and 7 the conductivity is given by

$$\sigma_{xx} + i\sigma_{xy} = \sigma_0 \int_0^\infty dt \exp[-i\omega_c t - S(t)], \tag{16}$$

where $S(t)=(e/mc)^2 \int_0^t dt'(t-t')F[2R_c \sin(\omega_c t'/2)]$. We substituted correlator (1) with parameters B_0 and ξ, extracted from comparison of such a correlator and experimental configuration of the RMF to Eq. (16), and numerically calculated σ_{xx} and σ_{xy}. After that we calculated magnetoresistance from Eqs. (9) and (10). The results of such calculations are shown in Fig. 5(a) (dashes). We can see that the value of the calculated negative MR is smaller by a factor of ~ 2 than $\Delta\rho_{xx}(B)/\rho_0$ measured in experiments. Taking into account the approximate character of the correlator (1), the agreement is satisfactory. We also can compare our experimental data with analytical results derived by different work[4] methods. Theory[7] predicts the following contribution to the negative magnetoresistance in the RMF:

$$\Delta\rho_{xx}(B)/\rho_0 \approx -1.5(\xi/R_c)^2 \ln(l/\xi) = -(\omega_c\tau_{tr})^2, \tag{17}$$

where $R_c = hmc/(e\lambda_F B_\perp)$, $\tau_{tr}=(\xi/v_F)[\ln(l/\xi)]^{0.5}$, and l is the mean free path in the RMF. Figure 5(a) shows the fit of Eq. (16) (squares) to the experimental results assuming $\ln(l/\xi)\simeq 1$ and $\xi \approx 0.3$ μm, which is a factor of ~ 2 smaller than the correlation length estimated from an antiferromagnetic (AFM) image. A good agreement with analytical expression (17) is achieved.

Finally, negative MR in the RMF has been calculated by Calvo[6] within the approach whereby the RMF was replaced by a space-homogeneous but time-dependent RMF. The problem has been solved analytically, and for $\omega_0\tau_{tr} \gg 1$ the following expression for the magnetoresistivity has been obtained:

$$\Delta\rho_{xx}(B)/\rho_0 \approx -(\omega_c/2\omega_0)^2, \tag{18}$$

where $\omega_0 = eB_0/mc$. Figure 5(a) shows the results of the comparison of our experimental data and the theoretical model considered in Ref. 6. Crosses are fits of Eq. (18) and yield the amplitude of the random magnetic field $B_0 = 0.64$ T, which corresponds to the value $B_0 = 0.05 B_{ext}$ in agreement with our estimations of the RMF amplitude. We point out that Eq. (18) can be obtained from Eq. (17) by replacing the transport scattering time, which is proportional to the correlation length, by $2\omega_0^{-1}$, thus proportional to the RMF amplitude. However, as was argued in Ref. 6, for a weak uniform perpendicular field, $\omega_0 \gg \omega_c$, the electron dynamics is determined by the RMF, therefore the transport scattering time is dependent on the RMF amplitude, and Eqs. (15), (17), and (18) are similar in the strong-RMF limit. Not knowing which approximation is more realistic, we may conclude that the value of the negative MR obtained in our experiments agrees by a factor of ~ 2 with the MR calculated in Refs. 4, 6, and 7.

In conclusion we have measured the magnetoresistance in the nonplanar ''hilllike'' 2DEG in the quasiparallel external magnetic field. Effectively due to the curved AlGaAs/GaAs interface, electrons move in a random magnetic field, when a uniform in-plane magnetic field is applied. Computer simulation of this effective inhomogeneous magnetic field for realistic curved 2DEG demonstrated that the RMF configuration is obtained when the in-plane field is directed along the direction perpendicular to the current flow. In such geometry we observed the negative MR, when the external magnetic field was tilted away from the plane of the substrate, and an additional perpendicular component of the magnetic field is applied to the system. Such observation agrees with a recent prediction of the quasiclassical negative MR in the RMF. Our experimental results support the idea that Boltzmann transport theory formulated in terms of the relaxation time fails in a long-range RMF. New semiclassical treatment of the transport beyond the relaxation-time approximation is applicable in a wide class of the systems, such as 2DEG in a random magnetic field.

The authors thank A.A. Quivy for the AFM image. This work is supported by FAPESP, CNPq (Brazilian agencies), and RFFI Grant Nos. 01-02-16892 and N 00-02-17896.

*Present address: Institute of Semiconductor Physics, Novosibirsk, Russia.

[1] P.A. Lee and T.V. Ramakrishnan, Rev. Mod. Phys. **57**, 287 (1985).
[2] H.W. Jiang, H.L. Stormer, D.C. Tsui, L.N. Pfeiffer, and K.W. West, Phys. Rev. B **40**, 12 013 (1989).
[3] B.I. Halperin, P.A. Lee, and N. Read, Phys. Rev. B **47**, 7312 (1993).
[4] D.V. Khveshchenko, Phys. Rev. Lett. **77**, 1817 (1996).
[5] A.D. Mirlin, J. Wilke, F. Evers, D.G. Polyakov, and P. Wolfle, Phys. Rev. Lett. **83**, 2801 (1998).
[6] M. Calvo, Phys. Rev. B **57**, R4241 (1998).
[7] A.D. Mirlin, D.G. Polyakov, and P. Wolfle, Phys. Rev. Lett. **80**, 2429 (1998).
[8] A.K. Geim, S.J. Bending, and I.V. Grigorieva, Phys. Rev. Lett. **69**, 2252 (1992).
[9] F.B. Mancoff, L.J. Zielinski, C.M. Marcus, K. Campman, and A.C. Gossard, Phys. Rev. B **53**, R7599 (1996).

[10] G.M. Gusev, U. Gennser, X. Kleber, D.K. Maude, J.C. Portal, D.I. Lubyshev, P. Basmaji, M. de P.A.Silva, J.C. Rossi, and Yu.V. Nastaushev, Surf. Sci. **361/362**, 855 (1996); Phys. Rev. B **53**, 13 641 (1996).

[11] G.M. Gusev, J.R. Leite, A.A. Bykov, N.T. Moshegov, V.M. Kudryashev, A.I. Toropov, and Yu.V. Nastaushev, Phys. Rev. B **59**, 5711 (1999).

[12] A.A. Bykov, G.M. Gusev, J.R. Leite, A.K. Bakarov, N.T. Moshegov, M. Casse, D.K. Maude, and J.C. Portal, Phys. Rev. B **61**, 5505 (2000).

[13] F. Evers, A.D. Mirlin, D.G. Polyakov, and P. Wolfle, Phys. Rev. B **60**, 8951 (1999).

[14] G.M. Gusev, A.A. Quivy, J.R. Leite, A.A. Bykov, N.T. Moshegov, V.M. Kudryashov, A.I. Toropov, and Yu.V. Nastaushev, Semicond. Sci. Technol. **14**, 1114 (1999).

[15] D.K.K. Lee, J.T. Chalker, and D.Y.K. Ko, Phys. Rev. B **50**, 5272 (1994).

[16] J.E. Muller, Phys. Rev. Lett. **68**, 385 (1992).

[17] M. Buttiker, Phys. Rev. B **38**, 9375 (1988).

[18] S.C. Zhang and D.P. Arovas, Phys. Rev. Lett. **72**, 1886 (1994).

[19] A.G. Aronov, A.D. Mirlin, and P. Wolfle, Phys. Rev. B **49**, 16 609 (1994).

[20] G.M. Gusev, P. Basmaji, Z.D. Kvon, L.V. Litvin, Yu.V. Nastaushev, and A.I. Toropov, J. Phys.: Condens. Matter **6**, 73 (1994).

[21] A.D. Mirlin, D.G. Polyakov, F. Evers, and P. Wolfle, Phys. Rev. Lett. **87**, 126 805 (2001).

[22] I.S. Ibrahim, V.A. Schweigert, and F.M. Peeters, Phys. Rev. B **56**, 7508 (1997).

[23] R. Menne and R.R. Gerhardts, Phys. Rev. B **57**, 1707 (1998).